Exact distribution of spacing ratios for random and localized states in quantum chaotic systems

S. Harshini Tekur,[1,*] Santosh Kumar,[2,†] and M. S. Santhanam[1,‡]

[1]*Indian Institute of Science Education and Research, Dr. Homi Bhabha Road, Pune 411 008, India*
[2]*Department of Physics, Shiv Nadar University, Gautam Buddha Nagar, Uttar Pradesh 201314, India*

Typical eigenstates of quantum systems, whose classical limit is chaotic, are well approximated as random states. Corresponding eigenvalue spectra are modeled through an appropriate ensemble described by random matrix theory. However, a small subset of states violates this principle and displays eigenstate localization, a counterintuitive feature known to arise due to purely quantum or semiclassical effects. In the spectrum of chaotic systems, the localized and random states interact with one another and modify the spectral statistics. In this work, a 3×3 random matrix model is used to obtain exact results for the ratio of spacing between a generic and localized state. We consider time-reversal-invariant as well as noninvariant scenarios. These results agree with the spectra computed from realistic physical systems that display localized eigenmodes.

I. INTRODUCTION

The generic eigenstates of quantum systems, whose classical limit is chaotic, display uniform probability density, except for featureless fluctuations [1,2]. Physically, this reflects the underlying irregular dynamics of a typical classical trajectory in agreement with the correspondence principle. It is also well known that the eigenvalues of consecutive generic eigenstates tend to repel one another in accordance with the Bohigas-Giannoni-Schmit conjecture [3] and the nature of this level repulsion is modeled through random matrix theory (RMT) [4,5]. This level repulsion property, encoded in the Wigner distribution of level spacings, has become popular as an indicator of quantum chaos.

Apart from generic states, a subset of eigenstates selectively displays pronounced enhancements of probability density, effectively localizing in configuration space. Depending on their physical origin, they could be scarred or, more generally, localized states. Scarring [6] is a striking quantum phenomenon in chaotic systems arising from quantum interferences that are reinforced in the vicinity of unstable periodic orbits and survive deep in the semiclassical regime [7]. On the other hand, the localized states such as bouncing ball modes in billiards [8,9] are induced by classical dynamical structures. In this paper, localized states denote any localized density enhancement irrespective of the underlying physical mechanism that creates it. In particular, RMT does not distinguish them based on their physical origins. Remarkably, the class of localized states modifies the spectral statistics by inducing deviations from the level repulsion property of chaotic systems [10,11].

Localized states were discovered in stadium billiards in 1979 [12] and since then they have been experimentally observed in a variety of chaotic systems including deformed microcavity lasers [13,14], quantum wells with chaotic electron dynamics [15], and hydrogen atoms in strong external fields [16]. Recently, scarring localization was also reported in Dirac fermions [17], strongly doped quantum wells [18], driven spin-orbit coupled cold atomic gases [19], a chaotic open quantum system [20], and an isomerizing chemical reaction [21]. Further, localized modes appear in spectral graph theory in relation to random graphs [22].

In a semiclassical sense, the generic eigenstates are associated with chaotic orbits, and localized states with the short time periodic orbits with time scales much shorter than the Heisenberg time $t_H \sim \hbar/\Delta$, where Δ is the mean level spacing. This is reflected in their spectral properties as well; nearest neighbor level spacings, s, of generic states are correlated and follow the Wigner distribution $P_W(s)$ whereas those of localized states are nearly uncorrelated and are closer to a Poisson distribution $P_p(s)$. Are the localized levels correlated with their neighboring generic levels? This has not been directly probed yet. In a spectrum containing both generic and localized states, deviations from $P_W(s)$, often modeled through use of the Brody distribution $P_B(s)$ [23], points to the existence of nontrivial correlations between them. This correlation quantifies the influence of localized states in the spectrum and indirectly characterizes the mixed nature of the underlying classical dynamics. This is even more useful for many-body systems, for which classical analogs may not exist but spacing distributions are widely used to characterize the spectral properties of metallic, insulating, many-body localized and thermal phases [24,25].

In the semiclassical limit as $\hbar \to 0$, the fraction of localized states tends to vanish and the spectrum is dominated by the generic states in accordance with the semiclassical eigenfunction hypothesis [1,26] and Schnirelman theorem [2]. Then, phenomenological distributions such as $P_B(s)$ become insensitive to the presence of a small subset of localized states. In these earlier approaches, the desired correlation signal is masked by the sheer statistical weight of the generic states.

*harshini.t@gmail.com
†skumar.physics@gmail.com
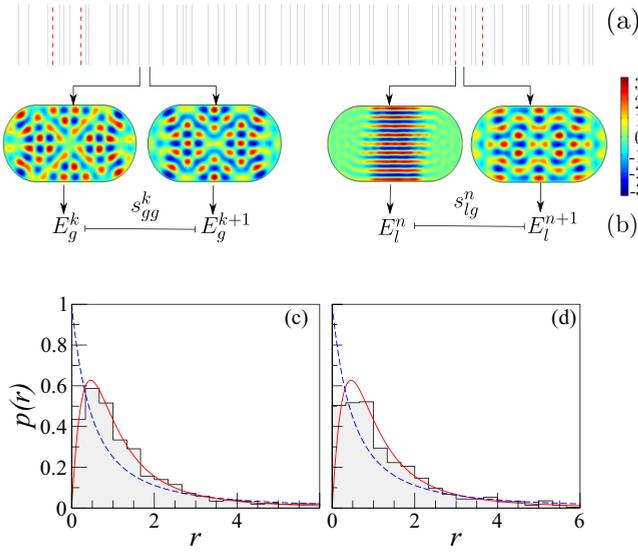‡santh@iiserpune.ac.in

FIG. 1. (a) Energy levels of stadium billiards. Scarred levels are marked in dashed (red) lines. A g-g type and g-l type spacing is shown. (b) Two consecutive generic eigenstates (state numbers 200 and 201), and two consecutive states (245 and 246) (a generic state next to a localized state). (c) Distribution of spacing ratios for g-g type spacings, (d) distribution of spacings for g-l type spacings. The red (solid) and blue (broken) lines are the standard results for $p_W(r)$ and $p_p(r)$ respectively.

II. RANDOM MATRIX MODEL

In this work, this hurdle is overcome by considering the level spacings s_{lg} *only* between localized and their neighboring generic states. Using a 3×3 random matrix model with a single parameter, for systems that preserve, and violate time-reversal symmetry, the exact distribution for the ratio of consecutive spacings [27,28] is obtained. This provides a robust characterization of the correlation between localized and generic states even as $\hbar \to 0$. The analytical results are compared with the random matrix simulations as well as results from two variants of stadium billiards [29], coupled quartic oscillator [30], and levels of samarium (Sm) atom [31]. We note that the ratio of spacing is a suitable statistic in this context since it does not require unfolding the spectrum.

The main motivation behind the random matrix model can be inferred from Fig. 1. A short sequence of energy levels of stadium billiards is displayed in Fig. 1(a) with localized states indicated by dashed lines. In Fig. 1(b) two pairs of consecutive eigenstates $|\Psi(x,y)|^2$ are shown: (i) consecutive generic states and we call the corresponding level spacing s_{gg} to be of g-g type and (ii) localized and its nearest neighbor generic state with spacing s_{gl} of g-l type. Such subsequences of levels are commonly encountered in quantum chaotic systems with mixed classical phase space, as well as in atomic and nuclear spectra [32,33]. Consider a chaotic quantum system whose Hamiltonian operator is $\widehat{H}$ and its energy spectrum is E_i, where $i = 1,2,\dots$ denotes the state number. The usual approach is to analyze all the level spacings in the spectrum. In contrast, in this work, we focus on the spacings s_{gl} between generic and localized states [Fig. 1(b)] defined as follows. From a sequence of consecutive energy levels $E_{k-1} < E_k < E_{k+1}$,

where one of them corresponds to a localized state, two spacings, $s_k = E_k - E_{k-1}$ and $s_{k+1} = E_{k+1} - E_k$, and hence one spacing ratio $r_k = s_k/s_{k+1}$ may be obtained, where at least one of the spacings is of the g-l type. Figure 1(c) shows the distribution of spacing ratio $p(r)$ obtained using only the generic levels (g-g type spacings) and in Fig. 1(d) for spacings involving a localized state (g-l type). For g-g type spacings, agreement with Wigner-type surmise

$$p_W(r) = \frac{1}{Z_\beta} \frac{(r + r^2)^\beta}{(1 + r + r^2)^{1+(3/2)\beta}} \tag{1}$$

(with $\beta = 1$ and $Z_\beta = \frac{8}{27}$) is clearly evident, whereas the g-l type spacings show marked, though weak, deviation from $p_W(r)$. Hence, the Hilbert space around a localized eigenstate can be locally modeled as a 3×3 Hamiltonian matrix.

Thus, we are led to consider an ensemble of 3×3 real-symmetric (for $\beta = 1$) or complex-Hermitian (for $\beta = 2$) random matrices H from the probability measure

$$\mathcal{P}(H)d[H] \propto \exp\left(-\frac{\beta}{2}\text{tr}\,\Sigma^{-2}H^2\right)d[H], \tag{2}$$

where 'tr' represents trace, $d[H]$ represents the product of differentials of all the independent parameters in the matrix elements, and $\Sigma = \text{diag}(1,1,\sqrt{\frac{k^2}{2-k^2}})$. Within the framework of Eq. (2), the random matrix is of the form

$$\mathbf{R_3} = \begin{bmatrix} H_{11} & H_{12} & H_{13} \\ H_{12} & H_{22} & H_{23} \\ H_{13} & H_{23} & H_{33} \end{bmatrix}, \tag{3}$$

where $0 \leqslant k^2 < 2$, and k is a parameter that represents the strength of coupling between a 2×2 Gaussian orthogonal ensemble (GOE) or Gaussian unitary ensemble (GUE) block and a 1×1 block representing a localized state. For systems with time-reversal symmetry (TRS), i.e., $\beta = 1$, the matrix elements are drawn from independent Gaussian distributions with mean zero and variances given as

$$\langle H_{11}^2 \rangle = \langle H_{22}^2 \rangle = 1, \quad \langle H_{33}^2 \rangle = \left(\frac{k^2}{2-k^2}\right),$$

$$\langle H_{12}^2 \rangle = \frac{1}{2}, \quad \langle H_{13}^2 \rangle = \langle H_{23}^2 \rangle = \frac{k^2}{2}. \tag{4}$$

For $\beta = 2$, corresponding to the broken time-reversal symmetry (TRSB) case, the matrix elements are Gaussian distributed with mean zero (real and complex for diagonal and off-diagonal), and variances given as

$$\langle H_{11}^2 \rangle = \langle H_{22}^2 \rangle = \frac{1}{2}, \quad \langle \text{Re}(H_{12})^2 \rangle = \langle \text{Im}(H_{12})^2 \rangle = \frac{1}{4},$$

$$\langle \text{Re}(H_{13})^2 \rangle = \langle \text{Im}(H_{13})^2 \rangle = \frac{k^2}{4},$$

$$\langle \text{Re}(H_{23})^2 \rangle = \langle \text{Im}(H_{23})^2 \rangle = \frac{k^2}{4},$$

$$\langle H_{33}^2 \rangle = \frac{1}{2}\left(\frac{k^2}{2-k^2}\right). \tag{5}$$

Physically, $0 \leqslant k \leqslant 1$ indicates the strength of correlation between localized and generic states. Thus, $k \ll 1$ implies

strong localization effects and might require semiclassical methods to understand its physical mechanism. On the other hand, $k \approx 1$ implies negligible localization and the RMT framework would be a suitable model. As $k \to 1$, the 3×3 matrix tends to that of standard Gaussian ensembles. In physical systems the localized and generic states are generally weakly coupled and we anticipate the coupling strength to be weak, i.e., $k \ll 1$. Hence, this weak coupling limit is the main regime of interest in this work. In this limit, H becomes the direct sum of a 2×2 GOE or GUE matrix (for $\beta = 1, 2$, respectively) and 0, the latter being also one of the eigenvalues and it notionally corresponds to the localized state.

III. DISTRIBUTION OF SPACING RATIOS

The main result of the paper, namely, the distribution $p(r)$ of spacing ratios r for the random matrix model defined in Eqs. (2)–(5), is obtained analytically in this section for the cases of $\beta = 1$ and $\beta = 2$.

A. $\beta = 1$ case

To derive an expression for $p(r)$, first the joint probability density of the eigenvalues $\{\lambda\}(\equiv \lambda_1, \lambda_2, \lambda_3)$ of the matrix model in Eq. (2) is obtained as

$$P(k; \{\lambda\}) \propto |\Delta(\{\lambda\})| \int_{O_3} d\mu(O) e^{-\text{tr}\Sigma^{-2}O^T\Lambda^2 O}, \quad (6)$$

where $\Lambda = \text{diag}(\lambda_1, \lambda_2, \lambda_3)$, $\Delta(\{\lambda\}) = |(\lambda_2 - \lambda_1)(\lambda_3 - \lambda_1)(\lambda_3 - \lambda_2)|$ is the Vandermonde determinant and $d\mu(O)$ represents the Haar measure over group O_3 of 3×3 orthogonal matrices with T being the transpose.

To calculate the ratio of consecutive spacings r we order them as $-\infty < \lambda_1 \leqslant \lambda_3$, $-\infty < \lambda_3 < \infty$, and $\lambda_3 \leqslant \lambda_2 < \infty$. Then, $r = (\lambda_2 - \lambda_3)/(\lambda_3 - \lambda_1)$. Moreover, the joint probability density for the ordered eigenvalues is given by $\widetilde{P}(k; \lambda_1, \lambda_2, \lambda) = 3! P(k; \lambda_1, \lambda_2, \lambda)$, where the intermediate eigenvalue $\lambda_3 = \lambda$.

Introducing $x = \lambda - \lambda_1$ and after some calculations whose details are in the Appendix, the distribution of r can be obtained as

$$p(k; r) = \frac{\sqrt{2 - k^2}}{\pi k^3} r(r + 1) \int_{-\infty}^{\infty} d\lambda \int_0^{\infty} dx \int_0^{\frac{\pi}{4}} d\phi \, x^4 \cos\phi$$

$$\times \exp\left\{-\frac{(2 + k^2)}{2k^2}\lambda^2 + \frac{1}{2}\left[\left(\frac{1}{k^2} - 1\right)\cos 2\phi + 1\right]\right.$$

$$\left. \times [2\lambda^2 - (\lambda - x)^2 - (\lambda + rx)^2]\right\}$$

$$\times I_0\left[\frac{x}{2}\left(\frac{1}{k^2} - 1\right)(r + 1)[2\lambda + (r - 1)x]\cos 2\phi\right]. \quad (7)$$

As $k \to 1$, the correct GOE result $p(1; r) = \frac{27}{8}\frac{r^2 + r}{(r^2 + r + 1)^{5/2}}$ is recovered as originally obtained in Ref. [28]. The limiting case $k \to 0$, relevant for the localized states of chaotic systems, is difficult to obtain using Eq. (7). However, starting from the joint probability density for $k = 0$ case, it is directly

obtained as

$$p(0; r) = \frac{1}{2\sqrt{2}}\left[\frac{(r + 1)}{(r^2 + 1)^{3/2}} + \frac{1}{[2r(r + 1) + 1]^{3/2}}\right.$$

$$\left. + \frac{r}{[r(r + 2) + 2]^{3/2}}\right]. \quad (8)$$

In particular, note that $p(0; r)$ is different from $p_p(r) = \frac{1}{(1+r)^2}$ obtained for the case of uncorrelated levels with the Poisson spacing distribution [27].

B. $\beta = 2$ case

For $\beta = 2$, the joint probability density of (unordered) eigenvalues turns out to be

$$P(k; \lambda_1, \lambda_2, \lambda_3) \propto \Delta^2(\{\lambda\}) \int_{\mathcal{U}_3} dU \exp(-\Sigma^{-2}U\Lambda^2 U^\dagger). \quad (9)$$

In this case, the unitary group integral can be performed using the Harish-Chandra-Itzykson-Zuber formula [34,35],

$$\int_{\mathcal{U}_N} dU \exp(-s\text{tr}XUYU^\dagger) = \prod_{m=1}^{N-1} m! \, (-s)^{-N(N-1)/2}$$

$$\times \frac{\det[\exp(-s\,x_j y_k)]_{j,k=1,\dots,N}}{\Delta(\{x\})\Delta(\{y\})}. \quad (10)$$

Here, dU is the Haar measure on unitary group $\mathcal{U}_N$, and $X = \text{diag}(x_1, \dots, x_N)$, $Y = \text{diag}(y_1, \dots, y_N)$.

After some calculations whose details may be found in the Appendix, the distribution of the ratio of spacings can be obtained as

$$p(k; r) = \frac{\sqrt{2 - k^2}}{4\pi k(1 - k^2)^2} r(r + 1) \sum_{j=1}^3 \left[\frac{b_j(5a_j^2 + 2b_j^2)}{a_j^4(a_j^2 + b_j^2)^2}\right.$$

$$+ \frac{3}{(a_j^2 + b_j^2)^{5/2}} \sinh^{-1}\left(\frac{b_j}{a_j}\right) - \frac{c_j(5a_j^2 + 2c_j^2)}{a_j^4(a_j^2 + c_j^2)^2}$$

$$\left. - \frac{3}{(a_j^2 + c_j^2)^{5/2}} \sinh^{-1}\left(\frac{c_j}{a_j}\right)\right]. \quad (11)$$

The forms of a_j, b_j, and c_j for $j = 1, 2, 3$ (which are functions of k and r) are rather unwieldy and shown in the Appendix. In the limit $k \to 0$, the exact result is obtained as

$$p(0; r) = \frac{1}{\pi}\left[\frac{r^2}{[r(r + 2) + 2]^2} + \frac{r(r + 2) + 1}{(r^2 + 1)^2}\right.$$

$$\left. + \frac{1}{[2r(r + 1) + 1]^2}\right]. \quad (12)$$

As anticipated, when $k \to 1$, the distribution in Eq. (11) coincides with the GUE result, obtained in Ref. [28], namely, $p(1; r) = \frac{81\sqrt{3}}{4\pi}\frac{(r^2 + r)^2}{(r^2 + r + 1)^4}$.
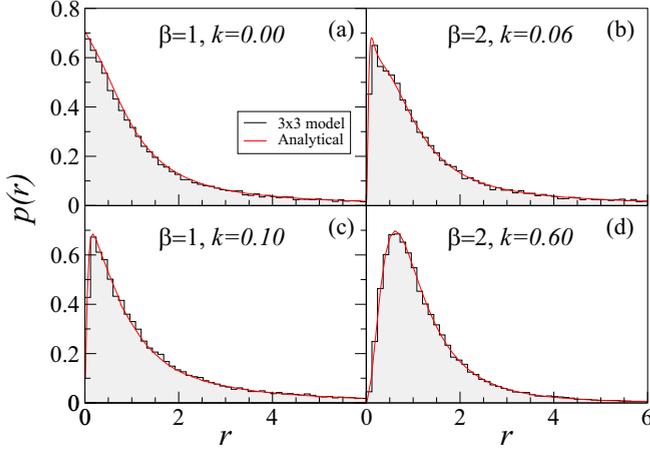
FIG. 2. Spacing ratio distribution, for g-l type spacings, obtained from random matrix simulations of 3×3 random matrices (histogram) compared with analytical $p(r)$ (red line). See text for how g-l type spacings are identified in simulations. The $\beta = 1$ and $\beta = 2$ cases are shown.

IV. NUMERICAL SIMULATION RESULTS

A. Random matrix model

In Fig. 2, the analytically obtained $p(r)$ in Eqs. (7) and (11) is compared with the results obtained by simulating an ensemble of 3×3 random matrices $\mathbf{R}_3$ following the prescription in Eqs. (2) and (4). The numerical simulations are performed by generating matrix elements with prescribed means and variances. If $k = 0$, $\mathbf{R}_3$ is block diagonal; one 2×2 block with eigenvalues λ_1, λ_2 and a 1×1 block with eigenvalue λ_3. The eigenvalue corresponding to a localized state is identified using the information entropy of an eigenstate [10]. The eigenvector corresponding to λ_i ($i = 1, 2, 3$) is $(a_{i,1}, a_{i,2}, a_{i,3})$. The corresponding information entropy is $S_i = -\sum_j |a_{i,j}|^2 \ln |a_{i,j}|^2$. For $k = 0$, the eigenvalue whose eigenvector is $(0,0,1)$ is far from a generic state and hence can be called a localized eigenvalue for our purposes. In this case, $S = 0.0$. As $k \to 1$, localized states typically disappear from the spectrum. If λ is the eigenvalue of the localized state identified using information entropy, then the spacing ratio is calculated as either $r = (\lambda - \lambda_2)/(\lambda_2 - \lambda_1)$, $r = (\lambda_3 - \lambda)/(\lambda - \lambda_1)$, or $r = (\lambda_3 - \lambda_2)/(\lambda_2 - \lambda)$, depending on whether the localized state corresponds to λ_3, λ_2, or λ_1 respectively. In Figs. 2(b) and 2(d), simulated histograms of $p(r)$ for $\beta = 2$ are shown and they display an excellent agreement with Eq. (11).

B. Applications to physical systems

The spacing ratio distribution for g-l type spacings is obtained for Hamiltonian systems whose classical limit is chaotic and hence their spacings are Wigner distributed, $P_W(s)$. The systems chosen for illustration are (i) the coupled quartic oscillator, (ii) computed levels of Sm atom, and (iii) stadium billiards ($\beta = 1$ and $\beta = 2$ variants). All of them contain localized eigenstates in their spectra. The computed distribution for g-l type spacing ratios agrees with the analytical results and in this k is treated as a fitting parameter.
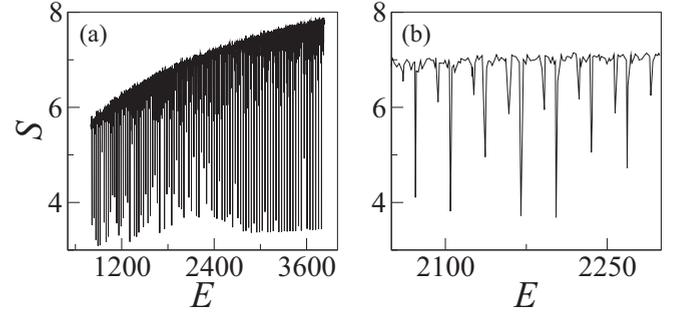

FIG. 3. (a) Information entropy S as a function of energy E for the coupled quartic oscillator system at $\alpha = 90$. The eigenstates having magnitude of information entropy $\lesssim 5.5$ can be identified as localized states. For the bulk of chaotic states that form the envelope, the value of S is consistent with the random matrix average for the information entropy (not shown here). (b) Enlarged view of a portion of (a), consisting of 175 states, out of which four may be considered to be localized.

1. Coupled quartic oscillator

In Fig. 4(a), the results are displayed for the coupled quartic oscillator, a well-studied model of quantum chaos [36]. The Hamiltonian for this system is

$$H = p_x^2 + p_y^2 + x^4 + y^4 + \alpha x^2 y^2, \qquad (13)$$

where α is the chaos parameter. The system becomes increasingly more chaotic as $\alpha \to \infty$. In this work, α is chosen to be equal to 90 such that the classical phase space is largely chaotic, with small regular regions due to the presence of a series of periodic orbits studied in detail in Ref. [37]. This is manifested in the corresponding quantum system as localized eigenstates, which are identified using information entropy. This is illustrated in Fig. 3 using the information entropy calculated for about 1800 states of the quartic oscillator at $\alpha = 90$. In Fig. 4(a), the computed distribution of g-l type spacings for the coupled quartic oscillator displays a good agreement with the analytical result shown in Eq. (7) with $k \approx 0.2$. As an independent verification, k can be extracted from the variance of the off-diagonal matrix elements (of Hamiltonian operator) locally around every localized state. For the quartic oscillator, both estimates agree with each other to within 30% error.
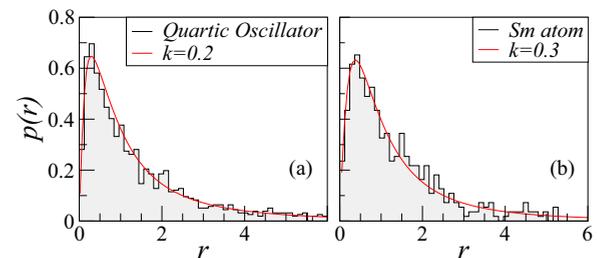

FIG. 4. Spacing ratio distribution, for g-l type spacings, obtained from systems whose classical limit is chaotic. Histograms are obtained from spectrum computed for (a) quartic oscillator and (b) levels of Sm from *ab initio* calculations. The solid (red) line is the fit obtained using the analytical relation in Eq. (7).
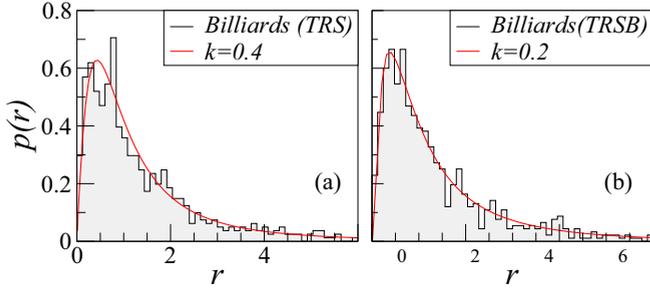
FIG. 5. Spacing ratio distribution, for g-l type spacings, obtained from systems whose classical limit is chaotic. Histograms are obtained from spectra computed for stadium billiards, with time-reversal symmetry (a) preserved ($\beta = 1$) and (b) broken ($\beta = 2$). The solid (red) line is the fit obtained using the analytical relation in Eqs. (7) and (11) for (a) and (b) respectively.

2. Sm atom

The application of random matrix theory in quantum chaos was first motivated by the study of spectral fluctuations in complex nuclei [38]. Lanthanide atoms, like samarium (Sm) have been studied in this context, using the multiconfiguration Dirac-Fock method to compute their spectra and identify localized states. Localization in this context is known to occur due to strong Coulomb mixing between configuration state functions having similar occupancy numbers of their subshells [39]. Figure 4(b) shows $p(r)$ for g-l type spacings in the computed levels of a lanthanide atom, namely, samarium (Sm). The energy levels of Sm exhibit complex configuration and mixing and were computed using the GRASP code [40]. The computed histograms of g-l type spacing ratios agree with $p(r)$ for $k \approx 0.3$.

3. Quantum billiards with and without time-reversal symmetry

The ratio distribution $P(r)$ for quarter stadium billiards is shown in Figs. 5(a) and 5(b), respectively, for TRS and TRSB cases. The eigenvalues for a closed quantum billiard system may be obtained by solving the Helmholtz equation

$$[\vec{\nabla}^2 + \mu^2]\vec{E} = 0, \tag{14}$$

with appropriate boundary conditions, where $\vec{E}$ is the electric field and μ the wave number. Localized and scarred states in billiards had been extensively investigated earlier [9,41–43] and deviations from $P_W(s)$ is attributed to such states, of which bouncing ball modes form a prominent class [44]. In Fig. 5(a), the simulated histogram of g-l type spacing for billiards agrees with the analytical result in Eq. (7) for $k \approx 0.4$. The TRSB case, corresponding to GUE results, is illustrated using a stadium billiard with a magnetized ferrite strip placed perpendicular to the two horizontal boundaries of the stadium. The TRS is broken by the phase shifts induced in the incident electromagnetic waves upon reflection from boundaries in the presence of a static magnetic field. This has been experimentally realized in microwave cavities [45,46] and has been simulated here with parameters taken from [45], modifying only the shape to a quarter stadium, in order to realize the bouncing ball modes, similar to the TRS case.

To compute the g-l type spacings, first the eigenspectra of this system were computed using a commercial finite-element method software, COMSOL Multiphysics [47]. Then, using the computed eigenvalues and normalized eigenvectors, i.e., the magnitude of the electric field E, the information entropy for each state is calculated using the relation $S_i = -\sum_j |E_{i,j}|^2 \ln |E_{i,j}|^2$, where j is the index for discretized position space. The localized states may be differentiated from the bulk of the chaotic states since the former have a significantly smaller magnitude of information entropy compared to the latter. Among all the localized states, bouncing ball modes are observed to be the most strongly localized, and hence the information entropy corresponding to these states has the least magnitude. Using the information entropy, the localized states are picked from the spectrum [as illustrated in Fig. 3(b)], and the required ratio distribution is determined. The result for $p(r)$ is shown as a histogram in Fig. 5(b) and it agrees with the analytical result [Eq. (11)] with $k \approx 0.2$.

V. CONCLUSION

To summarize, a typical spectrum of a chaotic quantum system has generic and localized eigenstates occurring as neighbors. Physically, they represent two distinct limiting behaviors. The former is modeled by random matrix assumptions and the latter deviates strongly from RMT based models. In this work, it is demonstrated that they display nontrivial correlations, quantified by the parameter k, the average strength of the Hamiltonian matrix element coupling these states. Physically, k is a measure of the strength of the correlation between localized and generic states.

This is a robust characterization that remains unaffected by the semiclassical limit in contrast to the phenomenological approach such as Brody distribution which had often been used to model the spectral transition from Poisson to GOE type statistics. In such an analysis, all the levels (localized and generic) are taken into account. Then, in the semiclassical limit of $\hbar \to 0$ or energy $E \to \infty$, localized modes ultimately would become a set of measure zero and the Brody distribution would nearly coincide with random matrix distributions. Hence, signatures of the localized states are masked by the large number of chaotic states. Thus, the Brody parameter being a single number representing this transition would become insensitive to the presence of localized modes in the semiclassical limit. In the approach presented in this paper, since the spacings (by construction) always involve at least one localized mode, the estimated value of k remains unaffected by the semiclassical limit.

Hence, the parameter k can be thought of as representing the coupling between a generic and a localized eigenstate and is sensitive even as $\hbar \to 0$. In this work, by considering a 3×3 random matrix model, an exact result is obtained for the distribution of the spacing ratio s_{lg} between a generic and a localized state. The analytical results are in good agreement with numerically computed spectra obtained from chaotic quantum systems such as billiards, coupled oscillator, and atomic spectra. In practice, it is not necessary to compute the localized states to estimate the value of the parameter k. For most physical systems which display localized states,

adiabatic methods can estimate the energies of localized states without computing the eigenvectors and information entropy. Such results exist for quartic oscillator [37,48] and stadium billiards [43]. A quantum stadium billiard has been experimentally realized and hence the results presented here can be experimentally verified as well.

APPENDIX: GENERALIZED GAUSSIAN ENSEMBLE AND RATIO OF CONSECUTIVE LEVEL SPACINGS

To derive the distribution of ratio of consecutive eigenvalue spacings, we need the joint probability density of the eigenvalues of the matrix model defined by Eq. (2). The cases of $\beta = 1$ and $\beta = 2$ are dealt with separately below.

1. $\beta = 1$ (2×2 GOE $\oplus$ Localized $\rightarrow$ 3×3 GOE)

The joint probability density of eigenvalues in this case follows as

$$P(k; \lambda_1, \lambda_2, \lambda_3) \propto |\Delta(\{\lambda\})| \int_{\mathcal{O}_3} dO \exp\left(-\frac{1}{2}\Sigma^{-2} O \Lambda^2 O^T\right), \tag{A1}$$

where the integral is over the group of 3×3 orthogonal matrices with dO representing the corresponding Haar measure. Also, $\Delta(\{z\}) = \prod_{j>k}(z_j - z_k) = \det[z_k^{j-1}]_{j,k=1,\ldots,N}$ is the Vandermonde determinant. For the unitary group, the celebrated Harischandra-Itzykson-Zuber formula [34,35] gives the result for this integral. Here we do not have such a result because Σ^{-2} and Λ^2 do not lie in the Cartan subalgebra corresponding to the orthogonal group. Nevertheless, for the three-dimensional case, it is possible to make progress using the recursive approach suggested by Guhr and Kohler [49]. Then, we have

$$\int_{\mathcal{O}_3} dO \exp(-s\mathrm{tr}XOYO^T) = \frac{1}{2\pi}\exp[-s(x_1+x_2+x_3)y_3] \int_{x_1}^{x_2} dx_1' \int_{x_2}^{x_3} dx_2' \frac{(x_2' - x_1')}{\left(-\prod_{\substack{j=1,2,3 \\ k=1,2}}(x_j - x_k')\right)^{1/2}}$$

$$\times \exp\left[-s(x_1' + x_2')\left(\frac{y_1+y_2}{2} - y_3\right)\right] I_0\left(\frac{s(x_1' - x_2')(y_1 - y_2)}{2}\right), \tag{A2}$$

where $I_0(z)$ is the modified Bessel function of the first kind and zeroth order [50]. This result cannot be used directly for Eq. (A1) since Σ^{-2} has two identical entries. We need to consider the limit $x_1, x_2 \rightarrow 1$. For this let us set $x_1 = 1 - \epsilon$ and $x_2 = 1$ and take the limit $\epsilon \rightarrow 0$. The crucial part in the above expression is

$$\lim_{\epsilon \to 0} \int_{1-\epsilon}^{1} dx_1' \frac{1}{[-(1-\epsilon-x_1')(1-x_1')]^{1/2}} = \lim_{\epsilon \to 0} \int_{1-\epsilon}^{1} dx_1' \frac{1}{[-(1-\epsilon-x_1')(1-x_1')]^{1/2}} = 2\lim_{\epsilon \to 0}\int_0^{\pi/2} d\theta, \quad \text{where } \epsilon \sin^2\theta$$

$$= 1 - x_1' = \pi.$$

The other occurrences of x_1' can be taken as 1. Now, using Eq. (A1), substituting $s = 1/2$, $x_3 = (2 - k^2)/k^2$, $y_1 = \lambda_1^2$, $y_2 = \lambda_2^2$, $y_3 = \lambda_3^2$, calling $x_2' = u$, and fixing the normalization the joint probability density of eigenvalues is obtained as

$$P(k; \lambda_1, \lambda_2, \lambda_3) = \frac{\sqrt{2-k^2}}{24\pi k^2\sqrt{1-k^2}}|(\lambda_2 - \lambda_1)(\lambda_3 - \lambda_1)(\lambda_3 - \lambda_1)|e^{-\left(\frac{2+k^2}{2k^2}\right)\lambda_3^2} \int_1^{2/k^2-1} du \frac{1}{\sqrt{2/k^2 - 1 - u}}$$

$$\times e^{-\frac{(u+1)}{4}(\lambda_1^2 + \lambda_2^2 - 2\lambda_3^2)} I_0\left(\frac{(u-1)}{4}(\lambda_1^2 - \lambda_2^2)\right). \tag{A3}$$

For calculating the ratio, the eigenvalues are restricted to the region defined by $-\infty < \lambda_1 \leqslant \lambda_3$, $-\infty < \lambda_3 < \infty$, $\lambda_3 \leqslant \lambda_2 < \infty$. The joint probability density of these ordered eigenvalues is then given by

$$\widetilde{P}(k; \lambda_1, \lambda_2, \lambda_3) = 3! P(k; \lambda_1, \lambda_2, \lambda_3). \tag{A4}$$

The probability density function of the ratio of consecutive spacings $r = (\lambda_2 - \lambda_3)/(\lambda_3 - \lambda_1)$ can then be found as

$$p(k; r) = \int_{-\infty}^{\infty} d\lambda_3 \int_{-\infty}^{\lambda_3} d\lambda_1 \int_{\lambda_3}^{\infty} d\lambda_2 \, \delta\left(r - \frac{\lambda_2 - \lambda_3}{\lambda_3 - \lambda_1}\right) \widetilde{P}(k; \lambda_1, \lambda_2, \lambda_3). \tag{A5}$$

Let us call $\lambda_3 = \lambda$ and define $x = \lambda - \lambda_1$ and $y = \lambda_2 - \lambda$, then the above integral, in terms of these new variables, becomes

$$p(k; r) = \int_{-\infty}^{\infty} d\lambda \int_0^{\infty} dx \int_0^{\infty} dy \, \delta\left(r - \frac{y}{x}\right) \times \widetilde{P}(k; \lambda - x, \lambda + y, \lambda). \tag{A6}$$

The δ function integral over y can be trivially done to yield

$$p(k; r) = \int_{-\infty}^{\infty} d\lambda \int_0^{\infty} dx \, x \widetilde{P}(k; \lambda - x, \lambda + rx, \lambda). \tag{A7}$$

Using Eq. (A3) in this, we obtain

$$p(k;r) = \frac{\sqrt{2-k^2}}{4\pi k^2 \sqrt{1-k^2}} r(r+1) \int_{-\infty}^{\infty} d\lambda \int_0^{\infty} dx \int_1^{2/k^2-1} du\, x^4 e^{-\frac{(2+k^2)}{2k^2}\lambda^2 + \frac{1}{4}(u+1)[2\lambda^2-(\lambda-x)^2-(\lambda+rx)^2]}\left(\frac{2-k^2}{k^2}-u\right)^{-1/2}$$

$$\times I_0\left(\frac{1}{4}x(u-1)(r+1)[2\lambda + (r-1)x]\right). \tag{A8}$$

It is found that the substitution $u = 1 + 2(1/k^2 - 1)\cos 2\phi$ leads to an expression which is comparatively more stable for numerical computation purposes:

$$p(k;r) = \frac{\sqrt{2-k^2}}{\pi k^3} r(r+1) \int_{-\infty}^{\infty} d\lambda \int_0^{\infty} dx \int_0^{\pi/4} d\phi\, x^4 \cos\phi\, e^{-\frac{(2+k^2)}{2k^2}\lambda^2 + \frac{1}{2}[(\frac{1}{k^2}-1)\cos 2\phi + 1][2\lambda^2-(\lambda-x)^2-(\lambda+rx)^2]}$$

$$\times I_0\left[\frac{1}{2}x\left(\frac{1}{k^2}-1\right)(r+1)[2\lambda + (r-1)x]\cos 2\phi\right]. \tag{A9}$$

2. $\beta = 2$ (2 × 2 GUE ⊕ Localized → 3 × 3 GUE)

The joint probability density of (unordered) eigenvalues in this case follows as

$$P(k;\lambda_1,\lambda_2,\lambda_3) \propto \Delta^2(\{\lambda\}) \int_{\mathcal{U}_3} dU \exp(-\Sigma^{-2} U \Lambda^2 U^{\dagger}). \tag{A10}$$

In this case, the unitary group integral can be performed using the Harish-Chandra-Itzykson-Zuber formula [34,35],

$$\int_{\mathcal{U}_N} dU \exp(-s\,\mathrm{str}\, XUYU^{\dagger}) = \prod_{m=1}^{N-1} m!\,(-s)^{-N(N-1)/2}\, \frac{\det[\exp(-s\, x_j y_k)]_{j,k=1,\ldots,N}}{\Delta(\{x\})\Delta(\{y\})}. \tag{A11}$$

Here, dU is the Haar measure on unitary group $\mathcal{U}_N$, and $X = \mathrm{diag}(x_1,\ldots,x_N)$, $Y = \mathrm{diag}(y_1,\ldots,y_N)$. If there is some multiplicity in the entries of X or Y, then we must use the above formula using proper limits. This is the case here, as Σ^{-2} has two identical entries, viz. 1. We find

$$P(k;\lambda_1,\lambda_2,\lambda_3) \propto (\lambda_2-\lambda_1)^2(\lambda_3-\lambda_1)^2(\lambda_3-\lambda_2)^2 \frac{\det\begin{bmatrix} e^{-\lambda_1^2} & -\lambda_1^2 e^{-\lambda_1^2} & e^{-(\frac{2-k^2}{k^2})\lambda_1^2} \\ e^{-\lambda_2^2} & -\lambda_2^2 e^{-\lambda_2^2} & e^{-(\frac{2-k^2}{k^2})\lambda_2^2} \\ e^{-\lambda_3^2} & -\lambda_3^2 e^{-\lambda_3^2} & e^{-(\frac{2-k^2}{k^2})\lambda_3^2} \end{bmatrix}}{\left(\lambda_2^2-\lambda_1^2\right)\left(\lambda_3^2-\lambda_1^2\right)\left(\lambda_3^2-\lambda_2^2\right) \det\begin{bmatrix} 1 & 0 & 1 \\ 1 & 1 & \left(\frac{2-k^2}{k^2}\right) \\ 1 & 2 & \left(\frac{2-k^2}{k^2}\right)^2 \end{bmatrix}}$$

$$\propto \frac{(\lambda_1-\lambda_2)(\lambda_2-\lambda_3)(\lambda_3-\lambda_1)}{(\lambda_1+\lambda_2)(\lambda_2+\lambda_3)(\lambda_3+\lambda_1)} \det\begin{bmatrix} e^{-\lambda_1^2} & \lambda_1^2 e^{-\lambda_1^2} & e^{-(\frac{2-k^2}{k^2})\lambda_1^2} \\ e^{-\lambda_2^2} & \lambda_2^2 e^{-\lambda_2^2} & e^{-(\frac{2-k^2}{k^2})\lambda_2^2} \\ e^{-\lambda_3^2} & \lambda_3^2 e^{-\lambda_3^2} & e^{-(\frac{2-k^2}{k^2})\lambda_3^2} \end{bmatrix}. \tag{A12}$$

On expanding the determinant and fixing the normalization factor, we get

$$P(k;\lambda_1,\lambda_2,\lambda_3) = -\frac{\sqrt{2-k^2}}{3\pi^{3/2}k(1-k^2)^2} \frac{(\lambda_1-\lambda_2)(\lambda_2-\lambda_3)(\lambda_3-\lambda_1)}{(\lambda_1+\lambda_2)(\lambda_2+\lambda_3)(\lambda_3+\lambda_1)} e^{-\lambda_1^2-\lambda_2^2-\lambda_3^2}\left[e^{-2(\frac{1}{k^2}-1)\lambda_1^2}\left(\lambda_2^2-\lambda_3^2\right) + e^{-2(\frac{1}{k^2}-1)\lambda_2^2}\left(\lambda_3^2-\lambda_1^2\right)\right.$$

$$\left. + e^{-2(\frac{1}{k^2}-1)\lambda_3^2}\left(\lambda_1^2-\lambda_2^2\right)\right]. \tag{A13}$$

Proceeding similar to the $\beta = 1$ case, we have Eq. (A7), but with $\widetilde{P}(k;\lambda_1,\lambda_2,\lambda_3)$ obtained from Eq. (A13). We find that

$$p(k;r) = \frac{2\sqrt{2-k^2}}{\pi^{3/2}k(1-k^2)^2} r(r+1) \int_{-\infty}^{\infty} d\lambda_3 \int_0^{\infty} dx\, [t_1(\lambda,x) + t_2(\lambda,x) + t_3(\lambda,x)], \tag{A14}$$

where

$$t_1(\lambda,x) = \frac{x^5 e^{-(1-r^2+\frac{2r^2}{k^2})x^2 + 2(1+r-\frac{2r}{k^2})x\lambda - (1+\frac{2}{k^2})\lambda^2}}{[(r-1)x+2\lambda](rx+2\lambda)}, \quad t_2(\lambda,x) = -\frac{(r+1)x^5 e^{-(1+r^2)x^2 + 2(1-r)x\lambda - (1+\frac{2}{k^2})\lambda^2}}{(-x+2\lambda)(rx+2\lambda)},$$

$$t_3(\lambda,x) = \frac{r\, x^5 e^{-(r^2+\frac{2}{k^2}-1)x^2 + 2(\frac{2}{k^2}-r-1)x\lambda - (1+\frac{2}{k^2})\lambda^2}}{(-x+2\lambda)[(r-1)x+2\lambda]}.$$

We notice that integrals involving t_1, t_2, t_3 are of a similar form, as given below:

$$\int_{-\infty}^{\infty} d\lambda \int_0^{\infty} dx \, \frac{x^5 e^{-\alpha^2 x^2 + 2\eta x\lambda - \gamma^2\lambda^2}}{(ux + 2\lambda)(vx + 2\lambda)} = \frac{\sqrt{\pi}}{8(v-u)} \left[\frac{b(5a^2 + 2b^2)}{a^4(a^2 + b^2)^2} + \frac{3\sinh^{-1}\left(\frac{b}{a}\right)}{(a^2 + b^2)^{5/2}} - \frac{c(5a^2 + 2c^2)}{a^4(a^2 + c^2)^2} - \frac{3\sinh^{-1}\left(\frac{c}{a}\right)}{(a^2 + c^2)^{5/2}} \right]. \quad \text{(A15)}$$

Here $a^2 = \alpha^2 - \frac{\eta^2}{\gamma^2}$, $b = \frac{\gamma}{2}(u + \frac{2\eta}{\gamma^2})$, $c = \frac{\gamma}{2}(v + \frac{2\eta}{\gamma^2})$. The integral converges for $\alpha^2 > 0$, $\gamma^2 > 0$, $\alpha^2\gamma^2 - \eta^2 > 0$. Hence, we can write down a closed form result for $p(k; r)$ based on this integral. Define

$$a_1 = \frac{\sqrt{2[1 + r(r+1)(2 - k^2)]}}{\sqrt{2 + k^2}}, \, a_2 = \frac{\sqrt{2[1 + r(r + k^2)]}}{\sqrt{2 + k^2}}, \, a_3 = \frac{\sqrt{2[2 + r(r + 2) - k^2(r + 1)]}}{\sqrt{2 + k^2}},$$

$$b_1 = \frac{k^2(3r + 1) - 2(r + 1)}{2k\sqrt{2 + k^2}}, \quad b_2 = \frac{2 + k^2(2r - 1)}{2k\sqrt{2 + k^2}}, \quad b_3 = \frac{2 - k^2(2r + 3)}{2k\sqrt{2 + k^2}}, \quad c_1 = \frac{k^2(3r + 2) - 2r}{2k\sqrt{2 + k^2}},$$

$$c_2 = \frac{k^2(r - 2) - 2r}{2k\sqrt{2 + k^2}}, \quad c_3 = \frac{2(r + 1) - k^2(r + 3)}{2k\sqrt{2 + k^2}}. \quad \text{(A16)}$$

Then the PDF for ratio of spacings is given by

$$p(k; r) = \frac{\sqrt{2 - k^2}}{4\pi k(1 - k^2)^2} r(r + 1) \sum_{j=1}^3 \left[\frac{b_j(5a_j^2 + 2b_j^2)}{a_j^4(a_j^2 + b_j^2)^2} + \frac{3}{(a_j^2 + b_j^2)^{5/2}} \sinh^{-1}\left(\frac{b_j}{a_j}\right) - \frac{c_j(5a_j^2 + 2c_j^2)}{a_j^4(a_j^2 + c_j^2)^2} \right.$$

$$\left. - \frac{3}{(a_j^2 + c_j^2)^{5/2}} \sinh^{-1}\left(\frac{c_j}{a_j}\right) \right]. \quad \text{(A17)}$$

It should be noted that the factor $(v - u)$ in the denominator of Eq. (A15) is $1, r + 1$, and r, respectively, for the integrals involving t_1, t_2, and t_3. The third one cancels the r factor in the numerator of Eq. (A 2), while the second one, when combined with $r + 1$ in the numerator of Eq. (A 2), leaves an overall negative sign. This sign has been absorbed in the definitions for b_2 and c_2 in Eq. (A16), noting that $\sinh^{-1} z$ in an odd function of z.

---

[1] M. V. Berry, J. Phys. A **10**, 2083 (1977).

[2] A. I. Shnirelman, Usp. Mat. Nauk. **29**, 181 (1974).

[3] O. Bohigas, M. J. Giannoni, and C. Schmit, Phys. Rev. Lett. **52**, 1 (1984).

[4] M. L. Mehta, *Random Matrices* (Academic, New York, 2004); T. Guhr, A. Müller-Groeling, and H. A. Weidenmüller, Phys. Rep. **299**, 189 (1998).

[5] P. J. Forrester, *Log-Gases and Random Matrices (LMS-34)* (Princeton University, Princeton, NJ, 2010).

[6] E. J. Heller, Phys. Rev. Lett. **53**, 1515 (1984).

[7] E. G. Vergini, Europhys. Lett. **110**, 10010 (2015).

[8] E. J. Heller and P. W. O'Connor, Nucl. Phys. B **2**, 201 (1987).

[9] B. Li and B. Hu, J. Phys. A **31**, 483 (1998).

[10] M. S. Santhanam and J. N. Bandyopadhyay, Phys. Rev. Lett. **95**, 114101 (2005); W. Li, L. E. Reichl, and B. Wu, Phys. Rev. E **65**, 056220 (2002).

[11] B. Batistic and M. Robnik, Phys. Rev. E **88**, 052913 (2013);

[12] S. Sridhar, Phys. Rev. Lett. **67**, 785 (1991).

[13] H. Cao and J. Wiersig, Rev. Mod. Phys. **87**, 61 (2015).

[14] J. Wiersig, Phys. Rev. Lett. **97**, 253901 (2006); S.-B. Lee, J.-H. Lee, J.-S. Chang, H.-J. Moon, S. W. Kim, and K. An, *ibid.* **88**, 033903 (2002); C.-H. Yi, S. H. Lee, M.-W. Kim, J. Cho, J. Lee, S.-Y. Lee, J. Wiersig, and C.-M. Kim, Phys. Rev. A **84**, 041803(R) (2011)

[15] P. B. Wilkinson, T. M. Fromhold, L. Eaves, F. W. Sheard, N. Miura, and T. Takamasu, Nature **380**, 608 (1996); see also related debate: T. S. Monteiro, D. Delande, and J.-P. Connerade, *ibid.* **387**, 863 (1997); T. M. Fromhold, F. W. Sheard, L. Eaves, and P. B. Wilkinson, *ibid.* **387**, 864 (1997).

[16] R. V. Jensen, M. M. Sanders, M. Saraceno, and B. Sundaram, Phys. Rev. Lett. **63**, 2771 (1989); D. Wintgen and A. Hönig, *ibid.* **63**, 1467 (1989); P. M. Koch, Chaos **2**, 131 (1992); D. Wintgen and H. Friedrich, in *Atomic Spectra and Collisions in External Fields 2*, edited by K. T. Taylor (Plenum, New York, 1988).

[17] H. Xu, L. Huang, Y.-C. Lai, and C. Grebogi, Phys. Rev. Lett. **110**, 064102 (2013).

[18] P. J. J. Luukko, B. Drury, A. Klales, L. Kaplan, E. J. Heller, and E. Räsänen, Sci. Rep. **6**, 37656 (2016).

[19] J. Larson, B. M. Anderson, and A. Altland, Phys. Rev. A **87**, 013624 (2013).

[20] D. Wisniacki and G. G. Carlo, Phys. Rev. E **77**, 045201(R) (2008).

[21] F. Revuelta, E. Vergini, R. M. Benito, and F. Borondo, J. Phys. Chem. A **120**, 4928 (2016); F. Revuelta, R. M. Benito, F. Borondo, and E. Vergini, *ibid.* **146**, 014107 (2017); F. Revuelta, E. Vergini, R. M. Benito, and F. Borondo, Phys. Rev. E **87**, 042921 (2013).

[22] A. V. Goltsev, S. N. Dorogovtsev, J. G. Oliveira, and J. F. F. Mendes, Phys. Rev. Lett. **109**, 128702 (2012); T. Martin, X. Zhang, and M. E. J. Newman, Phys. Rev. E **90**, 052808 (2014).

[23] T. A. Brody, Lett. Nuovo Cimento **7**, 482 (1973).

[24] R. Nandkishore and D. A. Huse, Annu. Rev. Condens. Matter Phys. **6**, 15 (2015); M. Serbyn and J. E. Moore, Phys. Rev. B **93**, 041424(R) (2016).

[25] V. E. Kravtsov, I. M. Khaymovich, E. Cuevas, and M. Amini, New J. Phys. **17**, 122002 (2015).

[26] A. Voros, in *Stochastic Behavior in Classical and Quantum Hamiltonian Systems* (Springer-Verlag, Berlin, 1979).

[27] V. Oganesyan and D. A. Huse, Phys. Rev. B **75**, 155111 (2007).

[28] Y. Y. Atas, E. Bogomolny, O. Giraud, and G. Roux, Phys. Rev. Lett. **110**, 084101 (2013).

[29] S. W. McDonald and A. N. Kaufman, Phys. Rev. Lett. **42**, 1189 (1979); G. Casati, F. Valz-Gris, and I. Guarnieri, Lett. Nuovo Cimento **28**, 279 (1980).

[30] O. Bohigas, S. Tomsovic, and D. Ullmo, Phys. Rep. **223**, 43 (1993).

[31] D. Angom and V. K. B. Kota, Phys. Rev. A **67**, 052508 (2003).

[32] M. G. Raizen, Adv. At. Mol. Opt. Phys. **41**, 43 (1999); Philos. Mag. B **80**, 12 (2000).

[33] H. A. Weidenmüller and G. E. Mitchell, Rev. Mod. Phys. **81**, 539 (2009).

[34] Harish-Chandra, Am. J. Math. **79**, 87 (1957).

[35] C. Itzykson and J.-B. Zuber, J. Math. Phys. **21**, 411 (1980).

[36] K. M. Atkins and G. S. Ezra, Phys. Rev. E **51**, 1822 (1995).

[37] M. S. Santhanam, V. B. Sheorey, and A. Lakshminarayan, Phys. Rev. E **57**, 345 (1998).

[38] E. P. Wigner, Ann. Math. **62**, 3 (1955).

[39] D. Angom and V. K. B. Kota, Phys. Rev. A **71**, 042504 (2005); M. S. Santhanam, J. N. Bandyopadhyay, and D. Angom, Phys. Rev. E **73**, 015201(R) (2006).

[40] K. G. Dyall, I. P. Grant, C. T. Johnson, F. A. Parpia, and E. P. Plummer, Comput. Phys. Commun. **55**, 425 (1989).

[41] B. Li, Phys. Rev. E **55**, 5376 (1997).

[42] J. Stein and H.-J. Stöckmann, Phys. Rev. Lett. **68**, 2867 (1992).

[43] A. Bäcker, R. Schubert, and P. Stifter, J. Phys. A **30**, 6783 (1997).

[44] M. Sieber, U. Smilansky, S. C. Creagh, and R. G. Littlejohn, J. Phys. A **26**, 6217 (1993).

[45] P. So, S. M. Anlage, E. Ott, and R. N. Oerter, Phys. Rev. Lett. **74**, 2662 (1995).

[46] H. Schanze, H.-J. Stöckmann, M. Martínez-Mares, and C. H. Lewenkopf, Phys. Rev. E **71**, 016223 (2005); B. Dietz, T. Friedrich, H. L. Harney, M. Miski-Oglu, A. Richter, F. Schäfer, and H. A. Weidenmüller, Phys. Rev. Lett. **98**, 074103 (2007).

[47] COMSOL Multiphysics Reference Manual, version 5.3, COMSOL, Inc, www.comsol.com.

[48] B. Eckhardt, G. Hose, and E. Pollak, Phys. Rev. A **39**, 3776 (1989).

[49] T. Guhr and H. Kohler, J. Math. Phys. **43**, 2707 (2002).

[50] M. Abramowitz and I. A. Stegun, *Handbook of Mathematical Functions: With Formulas, Graphs, and Mathematical Tables*, Vol. 55 (Courier, North Chelmsford, MA, 1964).